SELECTIVE HEAT SINTERING VERSUS LASER SINTERING: COMPARISON OF DEPOSITION RATE, PROCESS ENERGY CONSUMPTION AND COST PERFORMANCE

M. Baumers*, C. Tuck*, and R. Hague*

*3D Printing Research Group (3DPRG), Faculty of Engineering, University of Nottingham, Nottingham, NG7 2RD, UK

REVIEWED

Abstract

The Selective Heat Sintering (SHS) process has become available as a low cost alternative to Laser Sintering (LS) for the additive deposition of polymer objects. While both processes belong to the powder bed fusion variant of Additive Manufacturing (AM) technology, their operating principles vary significantly: SHS employs a thermal print head to selectively fuse material powder, whereas the LS approach utilizes a laser beam coupled with a galvanometer. Based on a series of build experiments, this research compares these technology variants along three dimensions of process efficiency: deposition rate (measured in cm³/h), specific process energy consumption (MJ/kg) and specific cost ($/cm³). To ensure that both platforms are assessed under the condition of efficient technology utilization, an automatic build volume packing algorithm is employed to configure a subset of build experiments. Beyond reporting absolute and relative process performance, this paper additionally investigates how sensitive the compared processes are to a variation in the degree of capacity utilization and discusses the application of different levels of indirect cost in models of low cost AM.

Introduction

As defined by the ASTM (2012), the term Additive Manufacturing (AM) describes a group of technologies capable of combining materials to manufacture complex products in a single process step. An important additional feature of the technology is that it permits the deposition of multiple components in parallel (Ruffo et al., 2006) and does so without the need for tooling of any kind (Hague et al., 2004). It has been noted that this one-step character lends AM technology with an unprecedented level of transparency in terms of raw material and energy consumption, and also cost (Baumers et al., 2013).

Above most other factors, the cost effectiveness of a new technology is a key determinant of technology adoption decisions for commercial applications (see, for example, Stoneman, 2002). To allow the ex-ante estimation of AM cost performance, a number of cost estimators have been developed for various additive processes (Alexander et al., 1998; Hopkinson and Dickens, 2003; Byun and Lee, 2006; Ruffo et al., 2006; Wilson, 2006; Munguia, 2009). As argued by Baumers et al. (2013), the assessment of AM cost and energy consumption can be structured alongside each other. By studying both aspects in conjunction, it is possible to implement a single methodology to make statements on both the private cost performance of the technology as well the environmental impact.

A recent development in the AM industry is the emergence of low cost additive platforms that aim to replicate the capability of more established processes, in the manufacture of complex components. According to Gibson et al. (2010), the recent wave of low cost AM

systems is due to the expiry of the protection of key items of intellectual property and patents. As part of an attempt an attempt to improve the understanding of the impact of this development in the area of powder bed fusion technology, which carries great significance for the additive manufacture of end-use products (Ruffo et al., 2006), this paper constructs an inter-process comparison of machine productivity, process energy consumption and financial cost. In this comparison, a Laser Sintering (LS) system is compared to the recently introduced Selective Heat Sintering (SHS) process.

As shown Figure 1, the SHS process operates by selectively fusing a thin layer of polymer powder via a thermal print head assembly. This assembly, which operates bidirectionally, incorporates thermal printheads (a), powder deposition mechanisms (b), and layer heaters (c). Material is built up in an internal build volume (d), the floor of which is a vertically movable build platform (e). Fresh powder is supplied via scoops to the powder deposition mechanism from powder containers (f). The print head assembly is separated from the build surface by a thermally conductive sheet (g). This sheet is fed from a fresh sheet roll (h) to a used sheet roll (i) during the process.
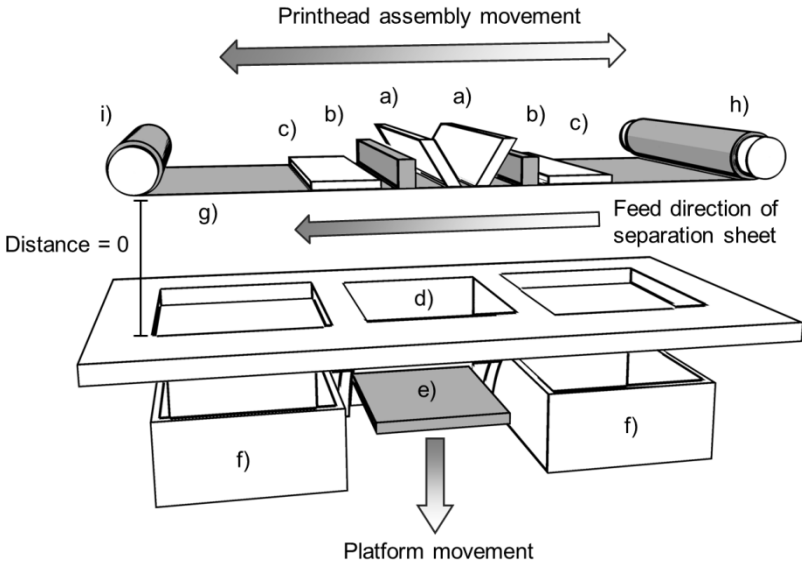

Figure 1: Schematic of the SHS process

Figure 2 shows a schematic diagram of LS. In LS, a laser system (a) is used to deflect a CO_2 laser beam to selectively sinter powder material. Fresh powder is gravity fed from powder containers (b) and infrared heating elements (c) are employed to preheat the build material. Before each preheating and exposure process a powder wiper (d) spreads a fine layer of powder over the build area (e), which is located over the vertically moveable build platform (f). Additional build volume heating is performed by resistance heating elements (g); excess unsintered material is discarded into overflow bins (h). Table 1 summarizes key characteristics of the investigated SHS platform, the Blueprinter, and the LS system, an EOSINT P100.
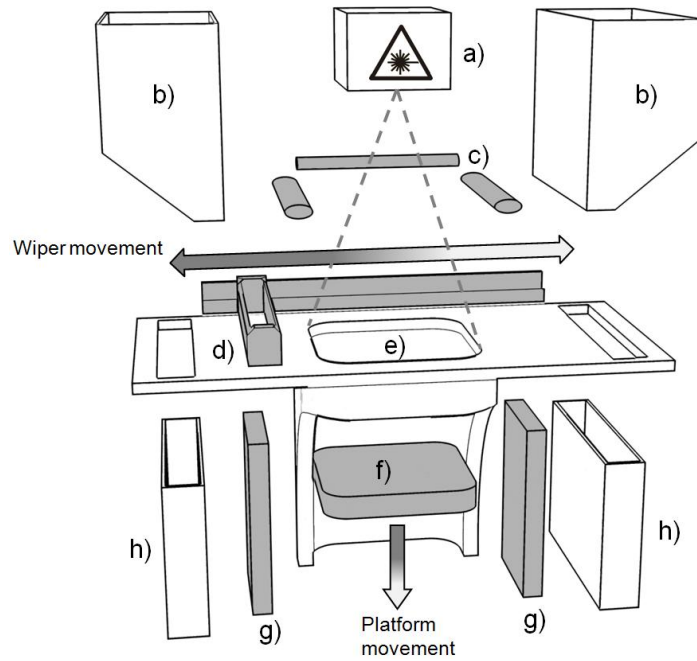
Figure 2: Schematic of the LS process
Image adapted from Baumers et al., 2011a

Table 1: Specifications of the investigated AM platforms

	Blueprinter	**EOSINT P100**
Manufacturer	Blueprinter ApS	EOS GmbH
Process type	Selective Heat Sintering	Laser Sintering
Energy deposition	Dual thermal print head	CO_2 laser, 30W
Usable build volume size (X / Y / Z)	160 × 140 × 150 mm	260 × 210 × 330 mm
Process atmosphere	Ambient atmosphere	N_2
N_2 source	None	N_2 generator, internal power supply
Heater type	Resistance	IR and resistance
Melting temperature	115 ºC	~173 ºC
Build material	SHS Nylon composite	PA2200
Used layer thickness	100 µm	100 µm
Support structures	Not required	Not required
Manufacturer reference	Blueprinter ApS (2015)	EOS GmbH (2015)

As a study of AM process economics and energy consumption, the overarching goal of this inter-process comparison is to implement a consistent methodology to generate useful summary metrics of machine productivity (in cm³/h), specific energy consumption (in MJ/kg), and the financial cost of normal build activity for both systems (in \$/cm³). It has been

demonstrated that powder bed fusion, in terms of energy consumption and cost, is sensitive to variation in degrees of capacity utilization (Baumers et al., 2011b). To provide some clarity as to whether SHS is sensitive to an underutilization of the available build capacity, as demonstrated for LS, this research performs two build experiments on both platforms: an initial single part build is performed to assess how well the platform performs if the available build volume in not fully used up and a second experiment reflecting a fully occupied build volume. As this paper forms a study of AM resource consumption, aspects relating to the mechanical performance, integrity, surface quality, material characteristics, build failure and post processing are omitted in this paper.

Methodology

The potential sensitivity of summary metrics of AM process performance to a variation of the degree of capacity utilization, implies that a consistent methodology should be applied to build experiments yielding such data. Thus, the experimental approach used in this paper is to record the process performance for the competing AM processes in two specifically designed build experiments:

- The initial build experiment performed on both systems analyses the deposition of a single test specimen in the available build space. To limit deviation from efficient technology operation, this geometry is located in the center of the available build space in the X/Y plane and as close to the build platform as possible.

- The second build investigates the performance of the AM platform for full capacity operation. Both SHS and LS allow the filling of the build volume via unconstrained three dimensional placement of parts, resulting in three dimensional packing configurations.

Due to AM platforms normally being single-machine electricity driven systems, the measurement of energy inputs to individual build experiments is not complex. Process energy consumption was recorded using a digital power meter (Yokogawa CW240) attached to the multi-phase or single phase AC power supply. Energy consumption was monitored throughout the entire build process, including any fixed process steps preceding and following the actual build activity. These could be for example, bed heating or energy consumption during machine's cool down phase. In terms of the recorded electricity consumption data, the focus lies on mean real power consumed per 1 second measurement cycle (measured in W) and the total cumulative electric energy consumed (measured in Wh).

The implementation of power monitoring experiments with consistent packing efficiency is based on a test part, as shown in Figure 3. Used in previous research, the 'spider' shape has been designed to have a relatively large footprint in the X/Y dimensions, thereby limiting overall packing density and enabling fast and economical experiments.
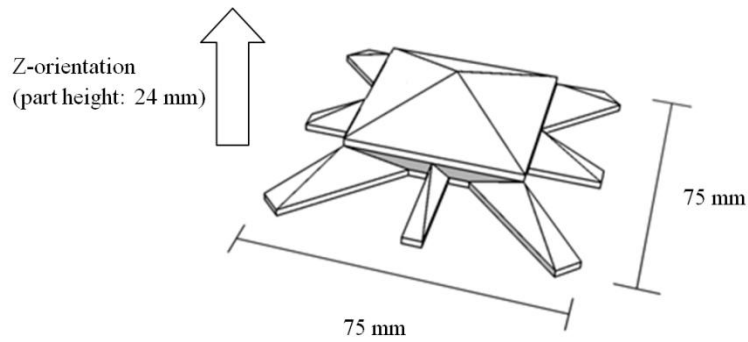
Figure 3: Spider-shaped test part

To further reduce the cost and time intensity of the experimental approach described in this paper, it was decided to limit the full build experiment to a fixed horizontal 'slice' of the build volume with a Z-height of 30 mm. To generate estimates for build time, process energy consumption and cost for full capacity utilization settings that exhaust the entire Z-height of both platforms (150 mm on the Blueprinter and 330 mm on the EOSINT P100), the experimental results of the full build experiment are subject to an extrapolation procedure in which the build height dependent aspects of the model are adjusted. In this process, no alterations were made to the fixed time and energy consumption increments resulting from system warm up and cool down, where applicable.

In contrast to the simplicity of the power monitoring setup, the design of build experiments featuring a comparable level of capacity utilization for both the Blueprinter and the EOSINT P100 required the use of an automated build volume packing algorithm. This allowed the definition of build configurations which are specific for each machine and involve an optimization procedure. To reflect the freedom of geometry inherent to both powder bed fusion processes, this algorithm was configured to freely place multiple instances of the test part shown in Figure 3 in the 3D build volume space and to flip the geometry upside down if this contributes to packing efficiency. Figure 4 shows the resulting full build configurations, with four test parts inserted in the Blueprinter's build volume and five test parts inserted into the EOSINT P100's build volume.
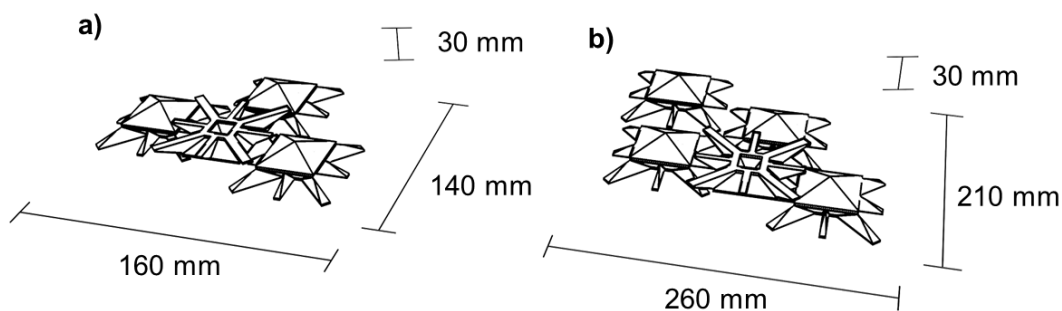

Figure 4: Blueprinter and EOSINT P100 full build specifications

Results and Discussion

The research approach selected for this inter-process comparison aims to meet three goals: firstly, it intends to present reliable experimental data on build time and process energy consumption. Secondly, it aims to specify and compare summary metrics based on full capacity utilization for machine productivity (deposition rate in cm³/h), process energy consumption (specific energy consumption in MJ/kg) and cost estimates derived from an appropriate cost model (specific cost in $/cm³). Thirdly, it aims to use these summary metrics of process efficiency to compare differences in the sensitivity of both platforms to capacity underutilization, which has been analyzed in financial terms (Ruffo et al., 2006) and for energy inputs (Baumers et al., 2011b). It is important to note that this study ignores any technical aspects relating to mechanical properties, material performance and deposition accuracy. Additionally, the cost model proposed below ignores any ill-structured costs associated with advanced manufacturing, such as those relating to build failure, error prevention, quality, machine setup, waiting time, idleness and inventory (see, for example, Son, 1991).

The experimental results reached in this study are reported in Table 2. As can be seen, both platforms required a considerable amount of time to complete each build experiment, ranging from 581.60 min for the single part build on the EOSINT P100 to 887.77 min required by the Blueprinter to complete the full build experiment, as shown above in Figure 4a. While the EOSINT P100 required extensive warm up procedures, ranging from 149.93 min to 184.92 min, and operator determined cool down times, ranging from 300.00 min to 480.00 min, the Blueprinter required only short system warm up times of 15.68 min for the single part build and 15.52 min for the full build, and no system cool down at all. At this point it is important to note that both platforms allow the operator to remove the build volume, also referred to as powder cake, after completion of the build for a rapid turnaround. This aspect is ignored in this study.

Due to the large amounts of unused machine capacity in both of the full build experiments, the deposition rates measured in the experiments are not reflective of efficient technology utilization and are therefore of little relevance for comparison to the literature. The same applies to the observed specific energy consumption rate. However, the build energy consumption rates, corresponding to mean real power consumption, observed on the EOSINT P100 (1,395 W and 1,420 W) correspond well to matching measurements from the literature (1,300 W, Kellens et al., 2010b). This indicates an accurate measurement setup.

Table 2: Experimental build time and power monitoring results

		Blueprinter		EOSINT P100	
		Single part	Full build	Single part	Full build
Build time and productivity	Total duration	659.00 min	887.77 min	581.60 min	833.64 min
	Warm up	15.68 min	15.52 min	149.93 min	184.92 min
	Deposition time	643.32 min	872.25 min	131.67 min	168.72 min
	Cool down*	N/A	N/A	300.00 min	480.00 min
	Deposition volume†	29.48 cm³	117.92 cm³	29.48 cm³	147.40 cm³
	Deposition rate	2.68 cm³/h	7.97 cm³/h	3.04 cm³/h	10.61 cm³/h
Energy consumption	Total energy consumption	15.14 MJ	20.71 MJ	33.41 MJ	42.44 MJ
	Warm up energy consumption	0.59 MJ	0.59 MJ	16.51 MJ	18.40 MJ
	Deposition process energy	14.55 MJ	20.13 MJ	11.01 MJ	14.37 MJ
	Cool down energy	N/A	N/A	5.88 MJ	9.66 MJ
	Deposition energy consumption rate	377 J/s	385 J/s	1,395 J/s	1,420 J/s
	Specific energy consumption†	466.88 MJ/kg	159.66 MJ/kg	1122.09 MJ/kg	285.07 MJ/kg

* Cool down duration based on operator discretion
† Estimated, assuming density of 1.01 g/cm³ (PA2200) and 1.1 g/cm³ (SHS Nylon composite)

The next step in the analysis is the extrapolation of the experimental results obtained in the full build experiments to the full Z-height of both machines. As described above, this is done by keeping process elements relating to warm up and cool down (where applicable) fixed and modifying the Z-height dependent process elements, which are net deposition time and deposition energy consumption, to match the systems' Z-height (150 mm on the Blueprinter and 330 mm on the EOSINT P100). This resulted in the addition of four extra 30 mm Z-increments containing an additional 16 parts on the Blueprinter and the addition of ten extra 30 mm Z-increments containing an additional 50 parts on the EOSINT P100. The extrapolated full capacity model is therefor based on a total deposition volume of 589.60 cm³ on the Blueprinter and a deposition volume of 1621.40 cm³ on the EOSINT P100. Table 3 reports results of the extrapolated model.

Table 3: Extrapolation of full build results to full capacity estimates

		Blueprinter	EOSINT P100
Extrapolated build time and productivity	Z-increments added	4	10
	Build time	4376.77 min	2520.84 min
	Deposition volume	589.60 cm³	1621.40 cm³
	Deposition rate	8.08 cm³/h	38.59 cm³/h
Extrapolated process energy consumption	Cumulative deposition process energy	100.65 MJ	158.07 MJ
	Total energy consumption	101.24 MJ	186.13 MJ
	Specific energy consumption†	156.10 MJ/kg	113.66 MJ/kg

† Estimated, assuming density of 1.01 g/cm³ (PA2200) and 1.1 g/cm³ (SHS Nylon composite)

As can be seen in Table 3, this analysis estimates the total deposition rate of the Blueprinter at 8.08 cm³/h, which is far slower than the deposition rate estimated for the EOSINT P100, at 38.59 cm³/h. This is also lower than the deposition rates reported for larger LS platforms at full capacity, ranging from 110.74 cm³/h estimated for an EOSINT P390 (Baumers, 2012) to 292.80 cm³/h reported for an EOSINT P760 (Kellens et al., 2010b). It should be noted that this result is sensitive to machine size and the overall level build volume utilization, which (in the extrapolated model) is estimated at 0.18 on the Blueprinter and 0.09 on the EOSINT P100. This is broadly comparable to volume utilization levels reported in other studies for LS, ranging from 0.04 (Baumers et al., 2011a) to 0.09 (Ruffo et al., 2006). The estimated specific energy consumption on the LS platform, 113.66 MJ/kg, is fully in line with the results from the literature, citing results of between 107.39 MJ/kg and 144.32 MJ/kg (Luo et al., 1999) and 129.73 MJ/kg (Kellens et al., 2010b). This indicates a high degree of validity for the extrapolation procedure. No comparable data were available in the literature for the Blueprinter.

The next step in this analysis is the construction of a cost model. Following the structure of existing activity-based cost models used for AM (Ruffo et al., 2006), the model employed is based on the idea of adding time dependent indirect costs to any incurred direct costs. Additionally, the model distinguishes between non-machine related indirect cost, made up of production overhead, administration overhead and labor, estimated at $17.16 per hour of machine operation, and machine costs including machine depreciation (straight line, 8 years) and machine maintenance and consumables. It should be noted that reliable data on machine maintenance and consumables is scarce, so this research applies a fixed machine purchase/annual maintenance cost ratio of 6.05%, as observed by Baumers et al. (2013), for both the Blueprinter and the EOSINT P100. Thus, the cost model estimates the total machine costs at $1.04 per hour of machine operation for the Blueprinter and at $7.95 per hour for the EOSINT P100.

As the Blueprinter has a smaller physical footprint and may not require workshop infrastructure and dedicated technician support, an alternative cost model is included which excludes the indirect cost rate identified above. Thus, the standard specification for the Blueprinter operates with a total indirect cost rate of 18.20 $/h and an alternative specification excluding such costs, resulting in a total indirect cost rate of 1.04 $/h. Based on this structure, and also reporting material costs and energy costs, Table 4 presents three alternative cost models.

Table 4: Cost model elements and comparison

	Blueprinter		Blueprinter, alt. cost model		EOSINT P100		Data source
	Single part	Full build	Single part	Full build	Single part	Full build	
Non-machine indirect cost rate	17.16 $/h		None		17.16 $/h		Adapted from Ruffo et al., 2006
Machine purchase	$27995.00				$214469.90		Own data
Depreciation period	8 years						Adapted from Ruffo et al., 2006
Annual operating time	5000 h						Adapted from Ruffo et al., 2006
Estimated cost rate of maintenance and consumables *	0.34 $/h				2.60 $/h		Own estimate
Total machine cost rate†	1.04 $/h				7.95 $/h		Own estimate
Total indirect cost rate	18.20 $/h		1.04 $/h		25.11 $/h		Own estimate
Total indirect costs	$199.91	$1327.68	$11.42	$75.86	$243.50	$1055.39	Own estimate
Material refresh ratio	0%				40%		Own estimate
Material consumption‡	0.03 kg	0.64 kg	0.03 kg	0.64 kg	0.42 kg	5.57 kg	Based on a Z-height of 30.00mm
Raw material price	53.90 $/kg				70.42 $/kg		Own data
Total material cost	$1.75	$34.96	$1.75	$34.96	$29.58	$392.24	Estimate based on net build volume size so likely to be an underestimation
Energy price	0.03 $/MJ						Own data
Energy costs	$0.45	$3.04	$0.45	$3.04	$1.00	$5.58	Own estimate
Total cost	$202.11	$1365.68	$13.62	$113.86	$274.08	$1453.21	Own estimate
Specific cost, per cm³	$6.86	$2.32	$0.46	$0.19	$9.30	$0.90	Own estimate
Specific cost, per part	$202.11	$68.28	$13.62	$5.69	$274.08	$26.42	Own estimate

* Based on a machine purchase/annual maintenance cost ratio of 6.05% adapted from Baumers et al. (2013)
† Sum of cost rate of maintenance, consumables and depreciation costs
‡ Based on a density for unconsolidated powder of 0.6 (Ruffo et al., 2006), and the usable build volume sizes listed in Table 1, assuming a cuboid build volume shape in both platforms

At this point, it is important to note that the presented cost model make significantly different assumptions about the powder refreshing on both systems. While the, somewhat unrealistic, assumption is made that the Blueprinter is able to reuse all of the material entering the build volume (implying in a material refresh ratio of 0%) the EOSINT P100 is assumed to require the removal and replacement of 40% of the material contained in its build volume after every build.

As shown in Table 4, the cost model leads to substantially different specific cost estimates across the two machines: for the Blueprinter the two alternative cost models result in total cost figures ranging from $13.62 for the single part build in the alternative configuration to $1365.68 for the full machine capacity build in the standard model. For the EOSINT P100, the cost model results in a total cost of $274.08 for the single part build and $1453.21 for the build at full machine capacity. Further using the full indirect cost model, the specific cost metric for the Blueprinter at full capacity utilization is estimated at 2.32 $/cm³. This compares unfavorably to the corresponding cost estimate for the EOSINT P100 of 0.90 $/cm³. However, once the reduced indirect cost level is applied to the Blueprinter, thereby implying that there are no overheads, infrastructure costs and labor expenses (which may or may not be the case), the specific cost metric drops to 0.19 $/cm³, which broadly matches the specific cost levels of 0.20 $/cm³ claimed by the machine vendor (Blueprinter ApS, 2015).

In terms of the aims formulated above for this paper, a full set of summary metrics on machine productivity, energy efficiency and cost can now be assembled. Figure 5 reports the results of this study in graphical form, suggesting that the investigated LS platform unambiguously has an advantage in terms of build speed (8.08 cm³/h versus 38.59 cm³/h). In terms of energy consumption, at least at full capacity utilization, the difference is not substantial, with the Blueprinter exhibiting a slightly higher specific energy consumption (156.10 MJ/kg against 113.66 MJ/kg). As discussed above, the summary cost metric suggests that the EOSINT P100 has a cost efficiency advantage (0.90 $/cm³ vs 2.32 $/cm³) if the higher indirect cost rate is applied to the Blueprinter. Implicitly, this assumes that both platforms require the same production floor setting and technician labor inputs, which may well not be the case and may amount to an inappropriate specification. If such costs are omitted, the Blueprinter performs more cost efficiently, resulting in a specific cost metric of 0.19 $/cm³.
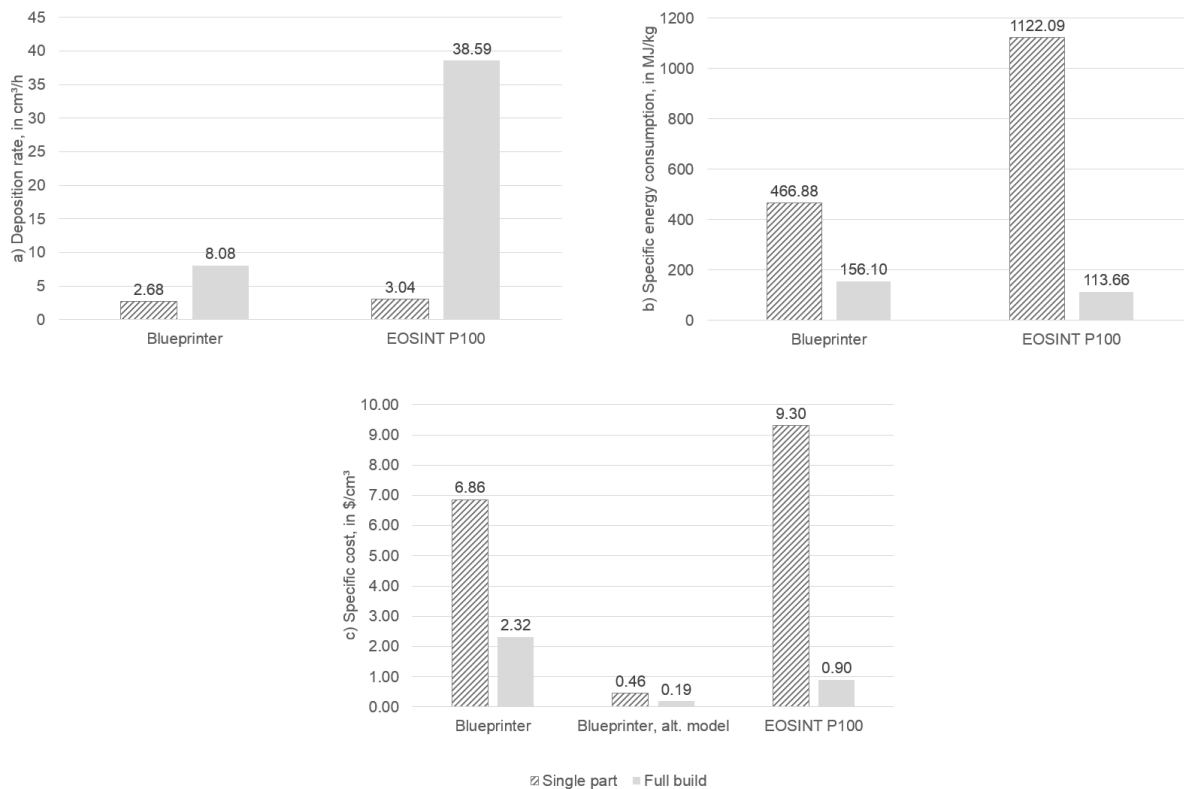
Figure 5: Comparing summary metrics of the combined model

Unambiguously, this research demonstrates that both the SHS and LS are highly sensitive to to the degree of machine capacity utilization, with all three types of metric (productivity, process energy and cost) benefitting substantially from the exploitation of the available Z-height and density of parts in the build volume, as discussed by Telenko and Seepersad (2010).

Conclusions

After presenting the results of the experimental portion of this research into resource consumption characteristics of the Blueprinter and the EOSINT P100, this paper has presented a set of summary metrics of system productivity, process energy consumption and specific cost. These metrics indicate that if an identical workshop setting and dedicated technician support is assumed, the EOSINT P100 appears to be at an advantage. Additionally, it is demonstrated that both platforms are sensitive to capacity underutilization. This highlights the requirement for methodologies that fill the available build volume, for example via automated build volume packing techniques.

Beyond this, the real insight gleaned in this research relates to cost model design. Low cost platforms such as Makerbot, Formlabs and also the Blueprinter are not designed for the production facility environment. Therefore cost models reflecting such an infrastructure (see, for example, Ruffo et al., 2006), including dedicated labor inputs, may be inappropriate. As observed in this research, the application of such a cost model, with high levels of indirect cost in particular, leads to high specific cost levels (2.32 $/cm³) despite the Blueprinter being marketed as a low cost AM system. For this reason, further research into methodologies capturing the value proposition of low cost AM systems is urgently required.

Acknowledgments

References

1. Alexander, P., Allen, S., and Dutta, D., 1998. Part orientation and build cost determination in layered manufacturing, Computer-Aided Design, 30 (5), pp. 343-356.

2. ASTM, 2012. "ASTM F2792 - 12e1 Standard Terminology for Additive Manufacturing Technologies," www.astm.org/Standards/F2792.htm.

3. Baumers, M., Tuck, C., Wildman, R., Ashcroft, I., Rosamond, R., and Hague, R., 2013. Transparency built-in: energy consumption and cost estimation for Additive Manufacturing, Journal of Industrial Ecology, 17(3) (2013) pp.418-431.

4. Baumers, M., 2012. Economic aspects of additive manufacturing: benefits, costs and energy consumption. PhD thesis. Loughborough University.

5. Baumers M., Tuck, C., Bourell, D., Sreenivasan, R., Hague, R., 2011a. Sustainability of additive manufacturing: measuring the energy consumption of the laser sintering process. Proceedings of the Institution of Mechanical Engineers Part B: Journal of Engineering Manufacture.225 (12), pp. 2228-2239.

6. Baumers, M., Tuck, C., Wildman, R., Ashcroft, I., and Hague, R., 2011b. Energy inputs to additive manufacturing: does capacity utilization matter?, Proceedings of the Solid Freeform Fabrication (SFF) Symposium 2011. The University of Texas at Austin.

7. Blueprinter ApS, 2015. [Corporate Website]. Available from: http://www.blueprinter.dk/ [Accessed: 01.07.2015].

8. Byun, H., Lee, K. H., 2006. Determination of the optimal build direction for different rapid prototyping processes using multi-criterion decision making, Robotics and Computer-Integrated Manufacturing, 22 (1), pp.69-80.

9. Munguia, F. J., 2009. RMADS: Development of a concurrent Rapid Manufacturing Advice System, Ph.D. thesis, Universitat Politecnica de Catalunya, Barcelona, Spain.

10. EOS GmbH, 2015. [Corporate Website]. Available from: http://www.eos.info/ [Accessed: 01.07.2015].

11. Gibson, I., Rosen, D., W., Stucker, B., 2010, Additive Manufacturing Technology – Rapid Prototyping to Direct Digital Manufacturing. Springer, New York.

12. Hague, R., Mansour, S., and Saleh, N., 2004. Material and design considerations for Rapid Manufacturing. *International Journal of Production Research*, 42 (22), pp. 4691-4708.

13. Hopkinson, N., and Dickens, P., 2003. Analysis of rapid manufacturing -using layer manufacturing processes for production. Proceedings of the Institution of Mechanical Engineers, Part C: Journal of Mechanical Engineering Science. 217 (C1), pp. 31-39.

14. Kellens, K., Dewulf, W., Deprez, W., Yasa, E., and Duflou, J., 2010a. Environmental analysis of SLM and SLS manufacturing processes. *Proceedings of LCE2010 Conference*. Hefei, China, 19 - 21.05.2010, pp. 423 -428.

15. Kellens, K., Yasa, E., Dewulf, W., Duflou, J., 2010b. Environmental Assessment of Selective Laser Melting and Selective Laser Sintering. *Going Green – CARE INNOVATION 2010*, Vienna, Austria, 8 – 11.11.2010.

16. Luo, Y., Ji, Z., Leu, M. C., and Caudill, R., 1999. Environmental Performance Analysis of Solid Freeform Fabrication Processes. *Proceedings of the 1999 IEEE International Symposium on Electronics and the Environment*, pp 1-6.

17. Ruffo, M., Tuck, C., and Hague, R., 2006. Cost estimation for rapid manufacturing – laser sintering production for low to medium volumes. *Proceedings of IMech E Part B: Journal of Engineering Manufacture*, 220(9), pp.1417-1427.

18. Son, Y. K., 1991. A cost estimation model for advanced manufacturing systems. International Journal of Production Research, 29(3), pp. 441-452.

19. Stoneman, P., 2002. The Economics of Technological Diffusion. Oxford: Blackwell.

20. Telenko, C., and Seepersad, C. C., 2010. Assessing Energy Requirements and Material Flows of Selective Laser Sintering of Nylon Parts. *Proceedings of the Solid Freeform Fabrication Symposium 2010*, Austin, USA, 8 – 10.08.2010, pp. 289-297.

21. Wilson, J. O., 2006. Selection for rapid manufacturing under epistemic uncertainty, Master's thesis. Georgia Institute of Technology, Atlanta, USA.